

RESEARCH

Open Access



# Knockdown of CDC20 promotes adipogenesis of bone marrow-derived stem cells by modulating $\beta$ -catenin

Yangge Du, Yunsong Liu, Yongsheng Zhou\* and Ping Zhang\* 

## Abstract

**Background:** Bone is a rigid organ that provides physical protection and support to vital organs of the body. Bone loss disorders are commonly associated with increased bone marrow adipose tissue. Bone marrow mesenchymal stromal/stem cells (BMSCs) are multipotent progenitors that can differentiate into osteoblasts, adipocytes, and chondrocytes. Cell division cycle 20 (CDC20) is a co-activator of anaphase promoting complex/cyclosome (APC/C), and is required for ubiquitin ligase activity. Our previous study showed that CDC20 promoted the osteogenic commitment of BMSCs and *Cdc20* conditional knockout mice suggested a decline in bone mass. In this study, we found that knockdown of *CDC20* promoted adipogenic differentiation of BMSCs by modulating  $\beta$ -catenin, which suggested a link between adipogenesis and osteogenesis.

**Methods:** Lentivirus containing a *CDC20* shRNA was used for *CDC20* knockdown in human BMSCs (hBMSCs). Primary mouse BMSCs (mBMSCs) were isolated from *Cdc20*<sup>fl/fl</sup> and *Sp7-Cre;Cdc20*<sup>fl/fl</sup> mice. Adipogenesis was examined using quantitative real-time reverse transcription PCR (qRT-PCR) and western blotting analysis of adipogenic regulators, Oil Red O staining, and transplantation into nude mice. *CDC20* knockout efficiency was determined through immunohistochemistry, qRT-PCR, and western blotting of bone marrow. Accumulation of adiposity was measured through histology and staining of bone sections. Exploration of the molecular mechanism was determined through western blotting, Oil Red O staining, and qRT-PCR.

**Results:** *CDC20* expression in hBMSCs was significantly decreased during adipogenic differentiation. *CDC20* knockdown enhanced hBMSC adipogenic differentiation in vitro. *CDC20*-knockdown hBMSCs showed more adipose tissue-like constructs upon hematoxylin and eosin (H&E) and Oil Red O staining. *Sp7-Cre;Cdc20*<sup>fl/fl</sup> mice presented increased adipocytes in their bone marrow compared with the control mice. mBMSCs from *Sp7-Cre;Cdc20*<sup>fl/fl</sup> mice showed upregulated adipogenic differentiation. Knockdown of *CDC20* led to decreased  $\beta$ -catenin levels, and a  $\beta$ -catenin pathway activator (lithium chloride) abolished the role of *CDC20* in BMSC adipogenic differentiation.

**Conclusions:** Our findings showed that *CDC20* knockdown enhanced adipogenesis of hBMSC and mBMSCs adipogenesis in vitro and in vivo. *CDC20* regulates both adipogenesis and osteogenesis of BMSCs, and might lead to the development of new therapeutic targets for “fatty bone” and osteoporosis.

\*Correspondence: kqzhouysh@hsc.pku.edu.cn; zhangping332@hsc.pku.edu.cn

Department of Prosthodontics, National Engineering Research Center of Oral Biomaterials and Digital Medical Devices, National Clinical Research Center for Oral Diseases, Beijing Key Laboratory of Digital Stomatology, Peking University School and Hospital of Stomatology, 22 Zhongguancun South Avenue, Haidian District, Beijing 100081, People's Republic of China



© The Author(s) 2022. **Open Access** This article is licensed under a Creative Commons Attribution 4.0 International License, which permits use, sharing, adaptation, distribution and reproduction in any medium or format, as long as you give appropriate credit to the original author(s) and the source, provide a link to the Creative Commons licence, and indicate if changes were made. The images or other third party material in this article are included in the article's Creative Commons licence, unless indicated otherwise in a credit line to the material. If material is not included in the article's Creative Commons licence and your intended use is not permitted by statutory regulation or exceeds the permitted use, you will need to obtain permission directly from the copyright holder. To view a copy of this licence, visit <http://creativecommons.org/licenses/by/4.0/>. The Creative Commons Public Domain Dedication waiver (<http://creativecommons.org/publicdomain/zero/1.0/>) applies to the data made available in this article, unless otherwise stated in a credit line to the data.

**Keywords:** CDC20, BMSCs, Adipogenesis, Bone marrow,  $\beta$ -catenin

## Background

Bone is a complex endocrine organ that facilitates structural support and protection of vital organs [1]. The majority of clinical conditions related to bone loss, including osteoporosis, aging, and hypercortisolism, are known to be accompanied by increased bone marrow fat [2–4]. This process involves the proliferation of BMSCs, their commitment to the adipogenic lineage, and their terminal differentiation [5]. BMSCs are multipotent progenitors giving rise to osteoblasts, adipocytes, and chondrocytes under specific stimulation [6]. As bone marrow adipocytes and osteoblasts share common progenitor cells, the lineage commitment of BMSCs must be dynamic [7]. Establishing a better understanding of fat storage and the osteoblast-adipocyte relationship within the bone marrow niche is necessary to elucidate the mechanisms underlying osteoporosis and age-related diseases.

The differentiation of BMSCs into adipocytes is driven by different transcription factors and regulated by various signaling pathways [6]. Extensive analyses have established the genetic cascade of adipogenesis. In response to adipocytic inducers, the transcription factors C/EBP $\beta$ , C/EBP $\delta$  and PPAR $\gamma$ 1 are rapidly activated in BMSCs and initiate the adipogenic cascade. This process includes elevated expression of two critical transcription factors responsible for adipogenesis, C/EBP $\alpha$  and PPAR $\gamma$ 2, followed by an increase in downstream genes characterized as mature adipocytes, including fatty acid binding protein 4 (FABP4) and adiponectin [8–13].

Cell division cycle 20 (CDC20) is the co-activator of anaphase-promoting complex/cyclosome (APC/C) [14]. CDC20 activates APC/C and promotes ubiquitin-dependent degradation of substrates [15]. In addition to participating in cell cycle progression, CDC20 was reported to be associated with many categories of cancers [16], brain development [17], and cellular apoptosis [18]. A high-fat diet is reported to lead to alteration of CDC20 level in pulmonary tissue [19]. The gene expression of *CDC20* was downregulated in obese women compared with that in the controls [20]. Thus, it seems that CDC20 correlates with adiposity; however, its role and mechanisms in BMSC adipogenesis remain elusive.

Our previous study revealed that CDC20 is a positive regulator of bone formation and osteogenesis of BMSCs [21]; and this study aimed to investigate its role in the adipogenic differentiation of BMSCs. To further explore whether CDC20 regulates adipogenesis of BMSCs, we used *CDC20* knockdown BMSCs and deleted the *Cdc20*

gene in osteoprogenitors using *Sp7-Cre* mice. The results presented that the levels of CDC20 decreased during the adipogenic differentiation of hBMSCs. Inhibition of CDC20 enhanced the adipogenic differentiation of hBMSCs through decreasing  $\beta$ -catenin expression. Furthermore, conditional knockout of *Cdc20* increased the number of adipocytes in bone marrow and the adipogenic differentiation of mBMSCs. This study provided new insights into how CDC20 manipulates the adipogenesis of BMSCs. Exploiting the potential of CDC20 in the BMSC differentiation process might become a new method to enhance bone mass as well as combat bone loss states.

## Materials and methods

### Cell culture

hBMSCs (No: 7500; Lots: 6899, 6881, 6890) and human adipose-derived stem cells (hASCs) (No: 7510; Lots: 2447, 8278, 8279) were purchased from ScienCell Research Laboratories (Carlsbad, CA, USA). Primary mBMSCs were separated from mice by flushing the bone marrow from the long bones. The detailed methods have been published previously [22]. BMSCs or ASCs were cultivated at 37 °C in 5% CO<sub>2</sub> conditions. They were cultivated in proliferation medium (PM), comprising penicillin/streptomycin, 10% (v/v) fetal bovine serum (FBS), and  $\alpha$ -minimum essential medium ( $\alpha$ -MEM) or Dulbecco's modified Eagle's medium (DMEM). The adipogenic medium (AM) included  $\alpha$ -MEM or DMEM added with 10  $\mu$ M insulin, 100 nM dexamethasone, 200  $\mu$ M indomethacin, 500  $\mu$ M 3-isobutyl-1-methylxanthine, penicillin/streptomycin, and 10% (v/v) FBS.

### Mice

*Cdc20<sup>fl/fl</sup>* and *Sp7-Cre;Cdc20<sup>fl/fl</sup>* mice were constructed by Biocytogen Co., Ltd (Beijing, China). Briefly, we first constructed *Cdc20<sup>fl/fl</sup>* mice using CRISPR-Cas9 system, and then mated them with *Sp7-Cre* mice to delete *Cdc20* in osteoprogenitors. The detailed information of conditional knockout mice in the experiments was reported in our previous work [21]. The primers are shown in Table 1.

### Lentivirus infection

Recombinant lentiviruses targeting *CDC20* were purchased in GenePharma Company (Shanghai, China). The lentivirus vectors contained the green fluorescent protein (GFP) gene and a puromycin-resistance gene. hBMSCs and hASCs were infected with lentiviruses using polybrene (5  $\mu$ g/ml) to enhance the transfection efficiency. Forty-eight hours later, puromycin (1 mg/ml) was utilized

**Table 1** Genotyping primers

<i>Cdc20</i> 5'loxP-F	CCTAAACTATGTGGAGTTCAAGGCCA	WT:202 bp
<i>Cdc20</i> 5'loxP-R	AGGATCTAGGATCTAGGTGACTCCC	Mut:321 bp
<i>Cdc20</i> 3'loxP-F	GAAGCAGCTCCTGTCTTGGAGTTGT	WT:405 bp
<i>Cdc20</i> 3'loxP-R	CCACAGCCTGGGTGGAATGGATAAA	Mut:490 bp
<i>Sp7-Cre</i> WT-F	TACCAGAAGCGACCACTTGAGC	263 bp
<i>Sp7-Cre</i> WT-R	CGCCAAGAGAGCCTGGCAAG	263 bp
<i>Sp7-Cre</i> Mut-F	TACCAGAAGCGACCACTTGAGC	445 bp
<i>Sp7-Cre</i> Mut-R	GCACACAGACAGGAGCATCTTC	445 bp

to select the infected cells. The oligonucleotide sequences mentioned are presented in Table 2.

**Oil red O staining**

BMSCs and hASCs were cultured in PM and AM, separately. At day 21, Oil red O staining was conducted. In brief, after flushing with phosphate-buffered saline (PBS), cells were fixed with 10% formalin. The cells were then rinsed with 60% isopropyl alcohol for 10 min and incubated with 0.3% Oil red O. After 100% isopropyl alcohol was added to the stained cells, quantitative measurement was conducted by determining their spectrophotometric absorbance at 520 nm.

**RNA isolation and qRT-PCR**

RNA was obtained using the TRIzol reagent (Invitrogen, Waltham, MA, USA). The RNA was reversed transcribed into cDNA using a PrimeScript RT Reagent Kit (Takara, Dalian, China). The cDNA was used as the template for the qPCR step of the qRT-PCR protocol using SYBR Green Master Mix (Roche Applied Science, Branchburg, NJ, USA). The expression of glyceraldehyde 3-phosphate

dehydrogenase (GAPDH) was used for normalization of qRT-PCR data. The  $2^{-\Delta\Delta Ct}$  method was used to analyze the relative gene expressions. The primers for indicated genes are shown in Table 2.

**Western blotting analysis**

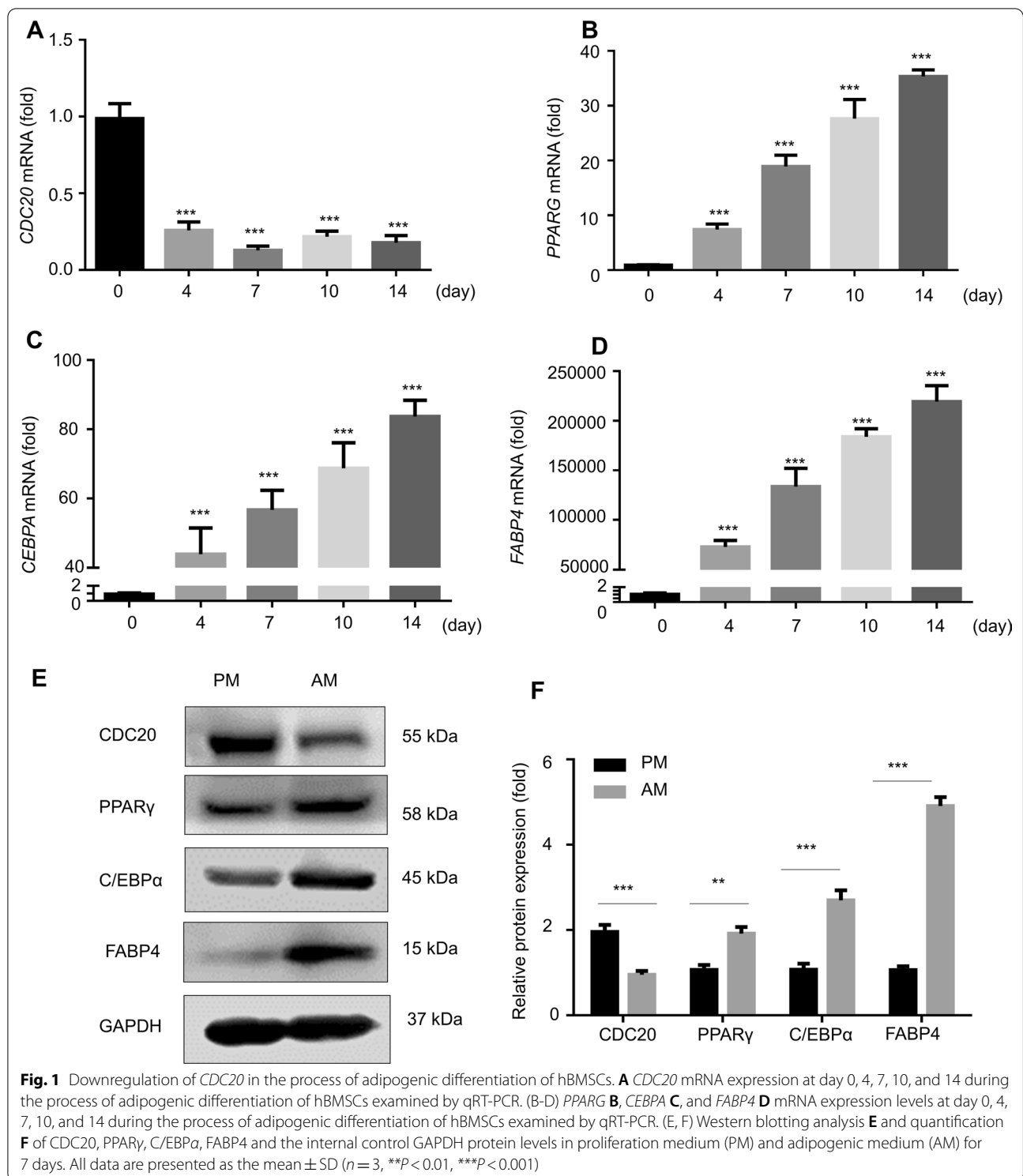
Cells were collected, washed with PBS and lysed using radioimmunoprecipitation assay (RIPA) lysis buffer with 2% protease inhibitor for 30 min. After centrifugation at  $12,000 \times g$  for 20 min, the isolated proteins were subjected to 10% or 15% SDS-PAGE and transferred to the PVDF membranes. After blocking in 5% dehydrated milk for 1–3 h, membranes were then incubated with primary antibodies against PPAR $\gamma$  (Abcam, Cambridge, MA, USA; 178,860), C/EBP $\alpha$  (Proteintech, Rosemont, IL, USA; 18,311–1-AP), fatty acid binding protein 4 (FABP4) (Proteintech; 12,802–1-AP), CDC20 (Abcam; ab183479), and  $\beta$ -catenin (Proteintech; 51,067–2-AP) overnight. Membranes were washed with PBS, incubated with the secondary antibody solution for 1 h, and then washed with PBS for three times. The immunoreactive protein bands were observed using an enhanced chemiluminescence (ECL) kit (CW BIO, Beijing, China). The protein levels were quantified through ImageJ software (National Institutes of Health, Bethesda, Maryland). GAPDH was used as internal control.

**In vivo adipose tissue formation**

BALB/c nude mice were purchased from the Vital River Corporation (Beijing, China). BMSCs were induced in AM for 1 week and then mixed with a Collagen Sponge for 2 h. The mixture was then transplanted under the subcutaneous space of the nude mice and then collected 6 weeks later for histological observation.

**Table 2** Sequences of RNA and DNA oligonucleotides

	Sense strand/ sense primer (5'-3')	Antisense strand/ antisense primer (5'-3')
Primers		
<i>GAPDH</i>	AAGGAGTAAGACCCTGGACCA	GCAACTGTGAGCAGGGGAGATT
<i>PPARG</i>	GAGGAGCCTAAGGTAAGGAG	GTCATTTCTGTTAAAGGCTGA
<i>CEBPA</i>	GGGCCAGGTCACATTTGTAAA	AGTAAGTCACCCCTTAGGGTAAGA
<i>FABP4</i>	CCTTAGATGGGGGTGTCCTGGT	GCCTTTCATGACGCATTCCACC
<i>CDC20</i>	TGTGTGGCCTAGTGTCTCTG	ACACCATGCTACGGCCTTGA
<i>Gapdh</i>	CAGGAGAGTGTTCCTCGTCC	TGAAGGGGTCGTTGATGGCA
<i>Cdc20</i>	CTCAAAGGACACACAGCACGG	CGCCACAACCGTAGAGTCTCA
<i>Pparg</i>	ACGGGCTGAGGAGAAGTCAC	TCACCGCTTCTTCAAATCTGTCT
<i>Cebpa</i>	ATTCTGCTTCTCTCGGGC	ACTGCCGGGATCTCAGCTTC
shRNA		
Control	TTCTCCGAACGTGTCACGT	
sh <i>CDC20</i> -1	GCACTGGACAACAGTGTGTAC	
sh <i>CDC20</i> -2	GCAGAAACGGCTTCGAAATAT	



### Immunocytochemistry

For immunofluorescence of bone sections, the fixed bone sections were blocked in 0.8% bovine serum albumin (BSA) for 1 h. Sections were incubated with the primary antibodies (1:200) against CDC20 (Abcam; ab183479) overnight, followed by incubation in 1:500 secondary antibody (ZF-0311, ZSGB-BIO, Beijing, China) for 1 h. Nuclei were stained using 4',6-diamidino-2-phenylindole (DAPI).

### Histology and staining

The femurs and tibiae of mice were fixed in phosphate-buffered formalin for subsequent experiments. They were decalcified in 0.5 M EDTA for 2 weeks and then divided into two parts. One part was prepared for Oil red O staining. The other part was dehydrated and embedded in paraffin for hematoxylin and eosin (H&E) staining.

### Statistical analysis

Data are shown given as the mean  $\pm$  standard deviation (SD). GraphPad Prism software (GraphPad Inc., San Diego, CA, USA) was utilized. Independent two-tailed Student's *t*-tests, one-way analysis of variance (ANOVA), and a Tukey's post hoc test were utilized to examine the level of significance. *P* values less than 0.05 were considered statistically significant.

## Results

### Downregulation of CDC20 in the process of adipogenic differentiation of hBMSCs.

To determine whether CDC20 participates in BMSC adipogenesis, we assessed its mRNA expression during the process of adipogenic induction. The qRT-PCR results revealed that CDC20 mRNA expression decreased significantly during adipogenic induction at day 0, 4, 7, 10, and 14 (Fig. 1A). Meanwhile, expression of the adipocyte regulator genes *PPARG*, *CEBPA*, and *FABP4* increased during adipogenic induction (Fig. 1B-D). Accordingly, western blotting analysis showed that adipocyte regulators PPAR $\gamma$ , C/EBP $\alpha$ , and FABP4 protein levels were upregulated, while CDC20 levels decreased during adipogenic induction of hBMSCs for 7 days (Fig. 1E, F).

### Knockdown of CDC20 enhances adipogenic differentiation of hBMSCs

To investigate the function of CDC20 in adipogenic differentiation, we constructed CDC20 stable knockdown hBMSCs. To assess the effect of CDC20 in other cell lines, we performed the experiments in human adipose-derived stem cells (hASCs). The CDC20 shRNAs and controls were transfected into hBMSCs and hASCs. Fluorescence staining showed that the lentiviral transduction efficiency was >90% (Fig. 2A, Additional file 1: SFig 1A). Similarly, the qRT-PCR results showed that CDC20 expression decreased dramatically after transfection (Fig. 2B, Additional file 1: SFig 1B). After cultivating hBMSCs and hASCs in AM for 21 days, CDC20 knockdown notably increased adipogenesis, according to Oil red O staining (Fig. 2C, D; Additional file 1: SFig 1C, D). *PPARG* and *CEBPA* mRNA expression increased significantly after adipogenesis was induced by CDC20 knockdown in hBMSCs (Fig. 2E, F). Western blotting revealed that PPAR $\gamma$  and C/EBP $\alpha$  protein levels increased after CDC20 silencing in adipogenic medium for 7 days (Fig. 2G, H).

### Knockdown of CDC20 promotes the formation of newly generated adipose tissue of hBMSCs

To further examine the adipogenic role of CDC20 in hBMSCs, we implanted hBMSCs with stable knockdown of CDC20 (shCDC20-1, shCDC20-2), or the negative control (NC), with a collagen scaffold, into nude mice. The newly generated tissue was gathered 6 weeks later. A diagram of this process is shown in Fig. 3A. The adipose tissue was further assessed by H&E staining and Oil red O staining, which revealed intracellular lipid accumulation. The shCDC20 groups generated more adipose-tissue-like positively stained complexes, while the NC group possessed fewer lipid droplets, as revealed by H&E and Oil red O staining (Fig. 3B).

### Conditional knockout of Cdc20 promotes adipogenesis in the bone marrow of mice

Next, we explored the effect of CDC20 on adipogenesis in vivo. We deleted *Cdc20* specifically from skeletal

(See figure on next page.)

**Fig. 2** Knockdown of CDC20 enhances adipogenic differentiation of hBMSCs. **A** Fluorescence micrographs showing the lentivirus transduction efficiency. Scale bar, 500  $\mu$ m. **B** CDC20 mRNA expression in control shRNA (NC) and CDC20 knockdown (shCDC20-1, shCDC20-2) groups examined using qRT-PCR. **C, D** Oil red O staining **C** and quantification **D** of hBMSCs after adipogenic induction for 21 days. Scale bar, 100  $\mu$ m. **E, F** Adipogenic regulators *PPARG* **E** and *CEBPA* **F** mRNA expression levels determined by qRT-PCR after adipogenic induction for 14 days. **(G, H)** Western blotting analysis **G** and quantification **H** of CDC20, PPAR $\gamma$ , C/EBP $\alpha$ , and the internal control GAPDH of negative control (NC) and CDC20 knockdown (shCDC20) cells in proliferation medium (PM) and adipogenic medium (AM) for 7 days. All data are presented as the mean  $\pm$  SD ( $n = 3$ , \*\* $P < 0.01$ , \*\*\* $P < 0.001$ )

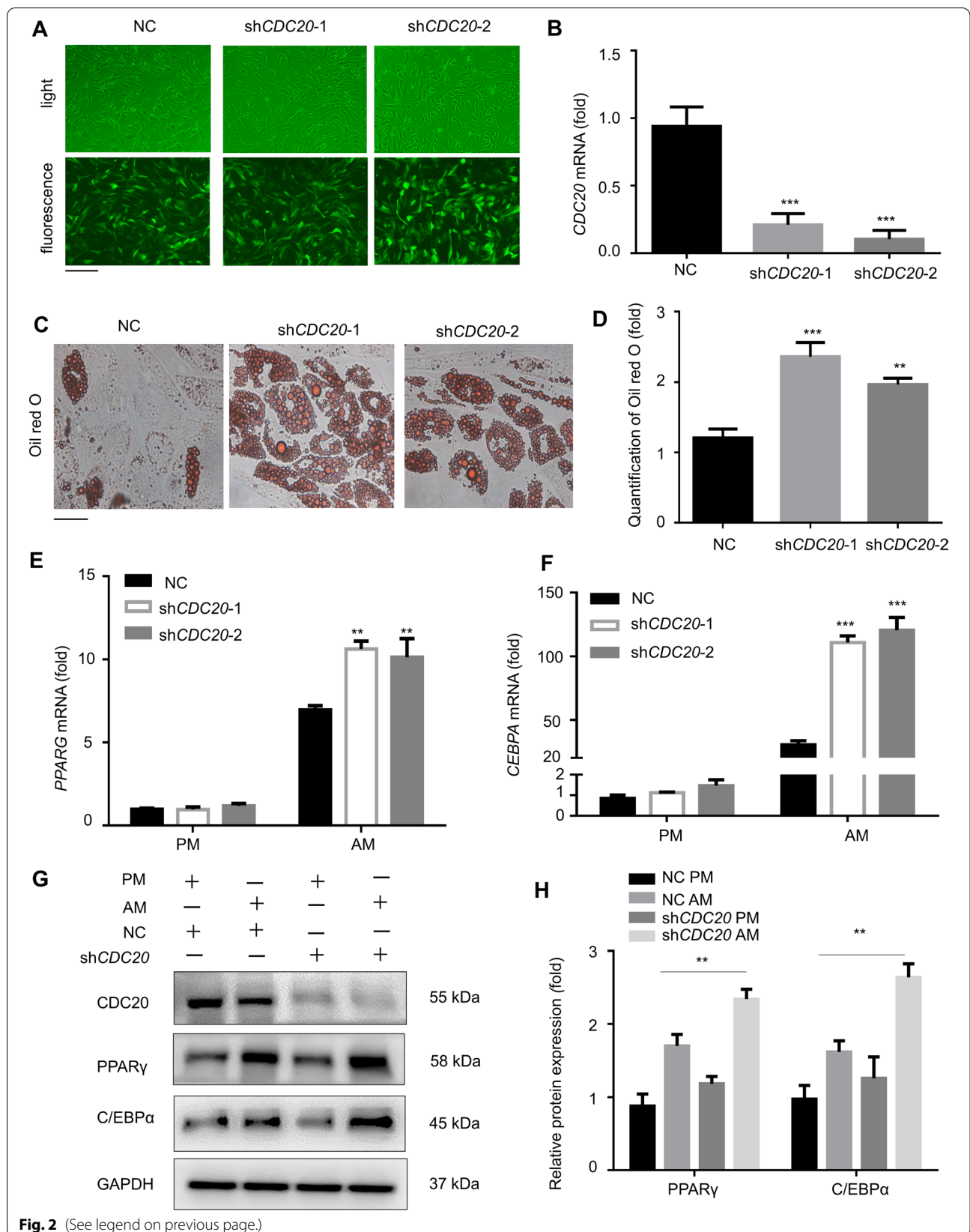


**Fig. 2** (See legend on previous page.)

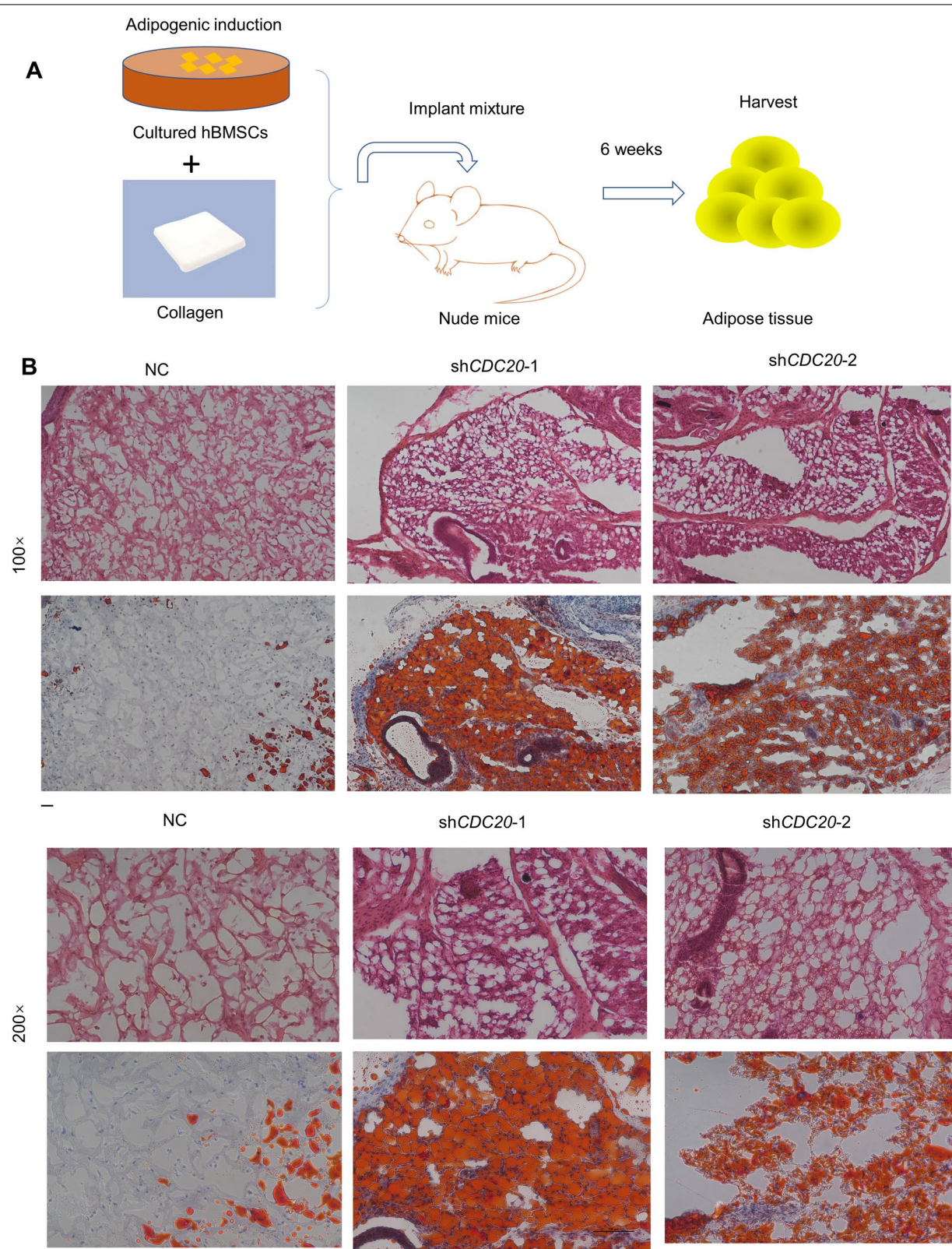


**Fig. 3** Knockdown of *CDC20* promotes the formation of newly generated adipose tissue of hBMSCs. **A** Schematic diagram demonstrating the procedure. **B** Oil red O staining and H&E staining in the NC, sh*CDC20*-1 and sh*CDC20*-2 groups. Scale bar, 50  $\mu$ m;  $n = 3$

tissue in our mouse model (Fig. 4A). The genotypes of constructed mice were examined (Fig. 4B). *Cdc20<sup>fl/fl</sup>* were the control mice, and *Sp7-Cre;Cdc20<sup>fl/fl</sup>* were the conditional knockout mice. In the femur sections of the mice, the *Cdc20* knockout efficiency in bone was measured using immunofluorescence (Fig. 4C). H&E staining of the femoral and tibial metaphysis of 6-week-old *Sp7-Cre;Cdc20<sup>fl/fl</sup>* mice presented increased numbers of adipocytes in the bone marrow compared with those in *Cdc20<sup>fl/fl</sup>* mice (Fig. 4D). The adipocytes were measured using ImageJ software, which determined the fat cell density as well as the fat tissue fraction. Dramatic differences were observed between *Cdc20<sup>fl/fl</sup>* and *Sp7-Cre;Cdc20<sup>fl/fl</sup>* mice (Fig. 4E), demonstrating that conditional knockout of *Cdc20* promoted the differentiation of mesenchymal stem cell and osteoprogenitors into adipocytes.

#### Conditional knockout of *Cdc20* increases adipogenic differentiation of mBMSCs

The mBMSCs were flushed out of mouse long bones and collected. The qRT-PCR results (Fig. 5A) and western blotting analysis (Fig. 5B) determined the knockdown efficiency. After adipogenic induction for 21 days, *Cdc20* deletion in mBMSCs significantly enhanced adipogenic differentiation, as determined by Oil red O staining and quantification (Fig. 5C, D). *Pparg* and *Cebpa* mRNA expression levels increased significantly following *Cdc20* deletion in mBMSCs (Fig. 5E, F), which demonstrated that conditional knockout of *Cdc20* increased mBMSC adipogenic differentiation.

#### Knockdown of *CDC20* decreases $\beta$ -catenin expression

To investigate the underlying molecular mechanisms of *CDC20*'s effect on the adipogenic differentiation of BMSCs, we examined signaling pathways related to adipogenesis. Interestingly, we found that the protein level of  $\beta$ -catenin decreased after knockdown of *CDC20* according to western blotting (Fig. 6A, B). Then, we activated Wnt/ $\beta$ -catenin signaling by adding LiCl. After adipogenic induction, Oil red O staining showed that LiCl treatment (5 mmol/L) decreased adipogenesis caused by knockdown of *CDC20* (Fig. 6C, D). Similarly, LiCl reduced the *PPARG* and *CEBPA* mRNA expression in *CDC20* knockdown BMSCs (Fig. 6E, F).

## Discussion

The imbalance between bone formation and resorption might contribute to various diseases, such as osteoporosis, osteopenia, and osteopetrosis [1]. Studies have demonstrated that the regulation of bone and fat mass are closely connected [23, 24]. The bone and fat in bone marrow were thought to show an inverse relationship. The anti-diabetic treatment, glitazone, was accompanied by bone loss, as well as increased bone marrow fat content [25]. Conditions with high bone mass resulting from mutant lipoprotein related receptor 5 (*Lrp5*) were accompanied by a decrease in bone mass [26]. Our previous studies have revealed that *CDC20* positively regulates BMSC osteogenesis [21], and in this study, we demonstrated its negative effect on adipogenesis.

*APC/C<sup>CDC20</sup>* recognizes the KEN box or D box of substrates to induce ubiquitination degradation, triggering the transition from metaphase to anaphase [27]. Studies have illustrated the effect of *CDC20* in hematopoietic stem cells [28]. It is expressed in the layers of the epidermis, and regulates the fate of adult stem cells [29]. In our study, the deletion of *Cdc20* reprogrammed the fate determination of osteoprogenitors and BMSCs, causing a shift from osteoblasts to adipocytes, which might partly lead to enhanced bone marrow adiposity accompanied by low bone mass in the conditional knockout mice.

Several factors and intercellular pathways have been claimed to control the fate of BMSCs [30]. Accumulating information has identified that adipose tissue can secrete various active molecules, including adiponectin, interleukin 6 (IL-6), and leptin [31]. Bones secrete various active cytokines, such as osteoprotegerin, osteocalcin, and osteopontin [32]. These cytokines have reciprocal roles in bone and fat metabolism. As one of the major regulators of adipogenesis, Wnt/ $\beta$ -catenin plays essential roles in cell differentiation, migration, and gene expression [33]. The connection between  $\beta$ -catenin and *CDC20* has been studied from many aspects. Silencing of *CDC20* inhibited the growth of prostate cancer by decreasing  $\beta$ -catenin levels [34, 35]. Knockdown of *CDC20* inhibited Wnt/ $\beta$ -catenin signaling through conducting during cell cycle [36]. In addition, knockdown of *CDC20* increased cell apoptosis and decreased their migratory ability by inhibition of the Wnt/ $\beta$ -catenin pathway [37]. In this

(See figure on next page.)

**Fig. 4** Conditional knockout of *Cdc20* promotes adipogenesis in the bone marrow of mice. **A** The design of the conditional deletion of the *Cdc20* gene. **B** Images of PCR genotypes of control (*Cdc20<sup>fl/fl</sup>*) and conditional knockout (*Sp7-Cre;Cdc20<sup>fl/fl</sup>*) mice. **C** Immunofluorescence of the relative expression of *CDC20* in bone sections of control (*Cdc20<sup>fl/fl</sup>*) and conditional knockout (*Sp7-Cre;Cdc20<sup>fl/fl</sup>*) mice. Scale bar, 100  $\mu$ m. **D** H&E staining of paraffin sections from femurs and tibiae of 6-week-old control (*Cdc20<sup>fl/fl</sup>*) and conditional knockout (*Sp7-Cre;Cdc20<sup>fl/fl</sup>*) mice. Scale bar, 100  $\mu$ m. **E** Quantification of fat cell density and fat tissue fraction based on the H&E staining of *Cdc20<sup>fl/fl</sup>* and *Sp7-Cre;Cdc20<sup>fl/fl</sup>* mice. All data are presented as the mean  $\pm$  SD ( $n = 3$ , \*\* $P < 0.01$ , \*\*\* $P < 0.001$ )

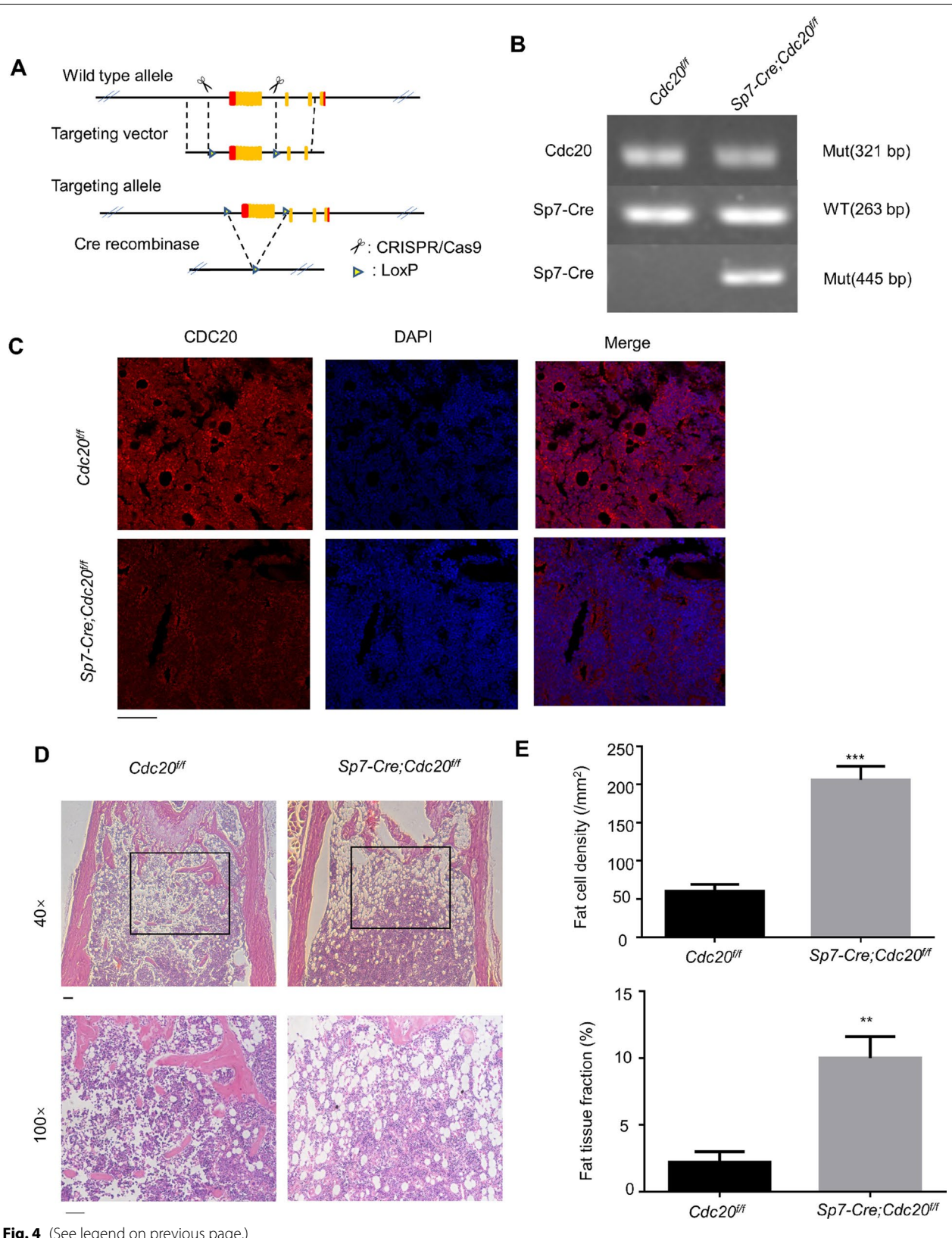
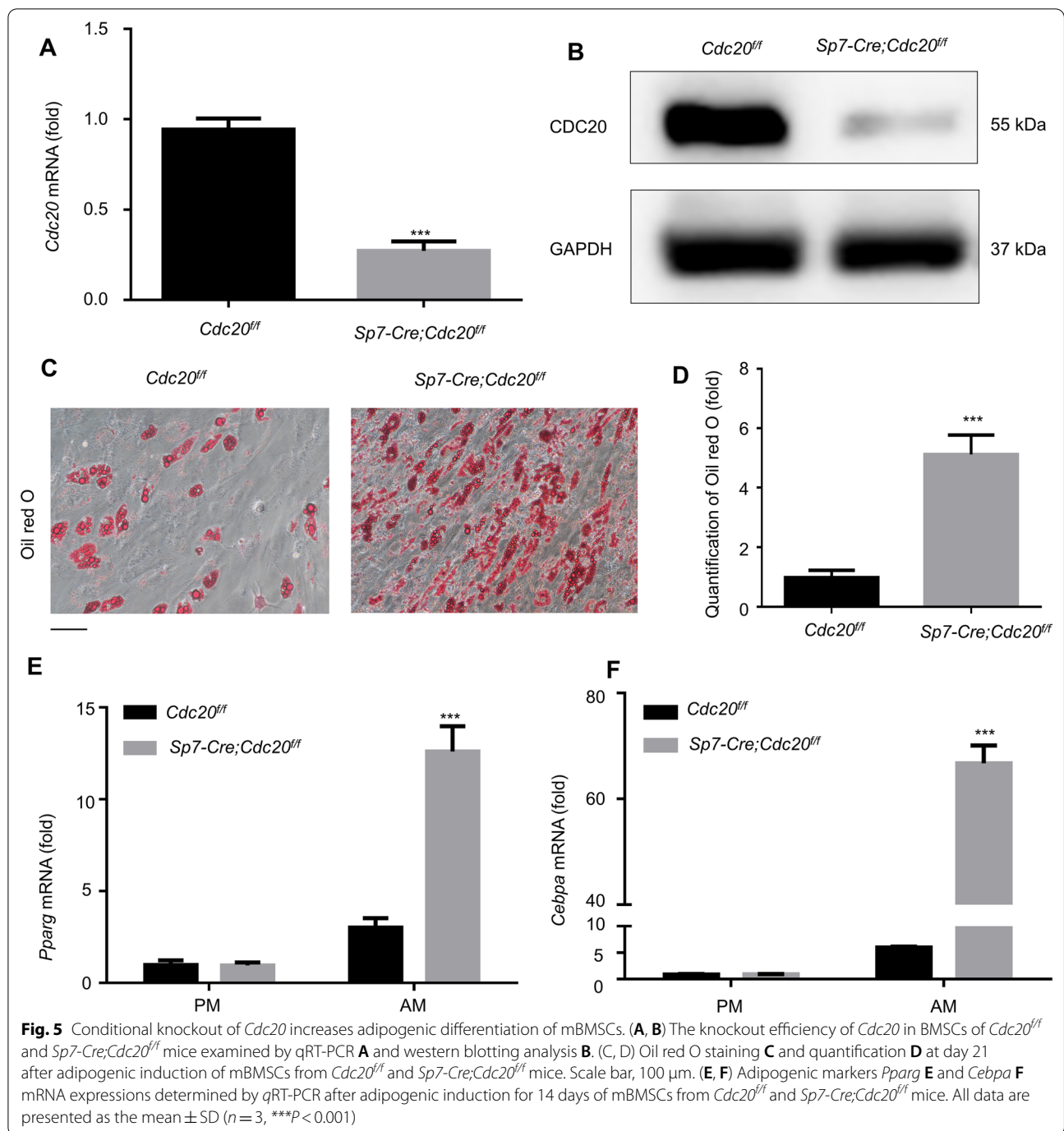


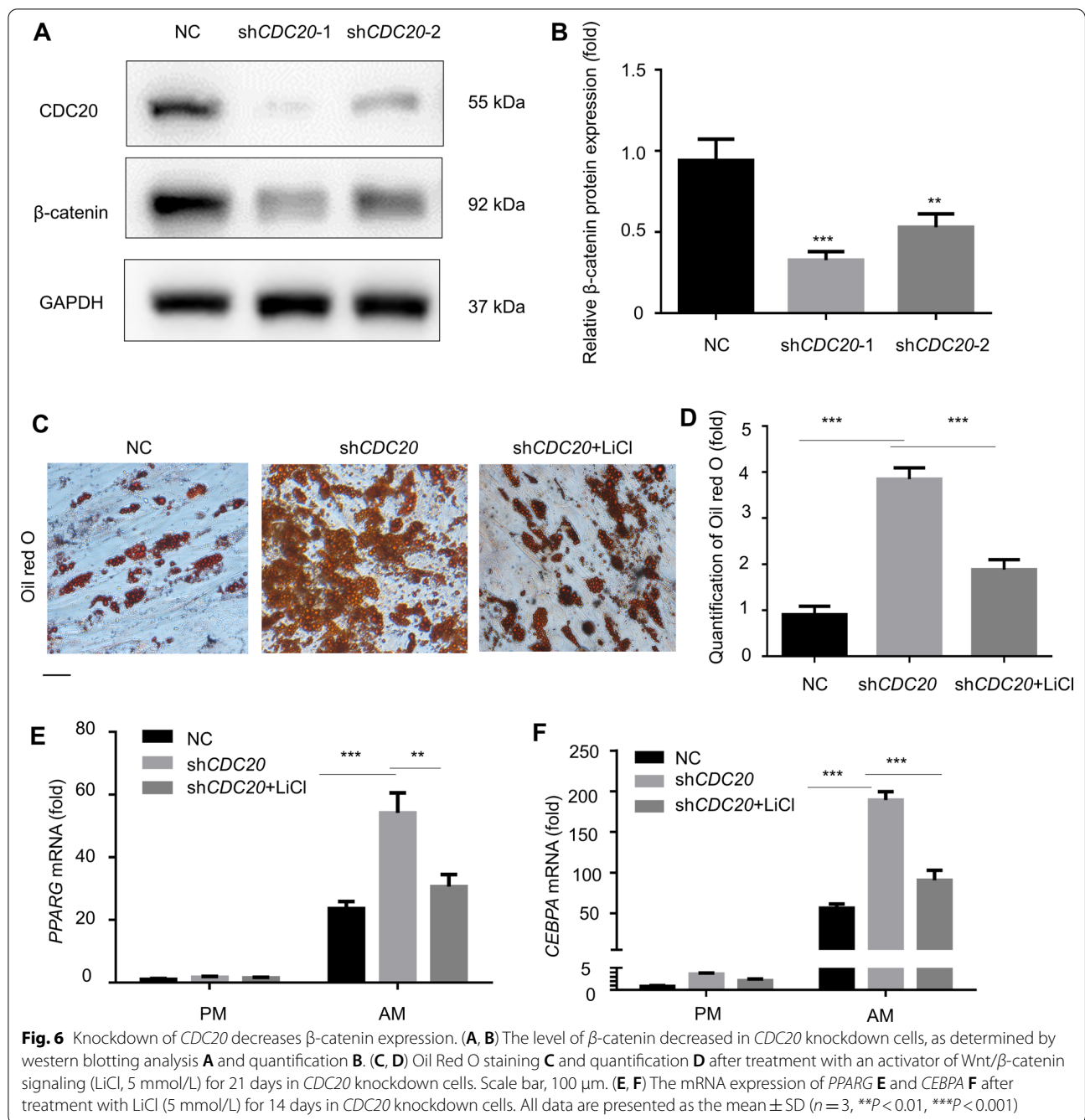
**Fig. 4** (See legend on previous page.)



study, we demonstrated that CDC20 inhibited the adipogenic differentiation of BMSCs by regulating  $\beta$ -catenin, which provides evidence for the manipulation of bone marrow fat.

Using conditional knockout mice constructed through the Cre/LoxP system driven by *Sp7-Cre* [38], our lineage tracing showed that *Cdc20* deletion from osteoprogenitors

induced them to become adipocytes in the bone marrow microenvironment. Other researchers used *Osx* (Osterix, also known as *Sp7*)-*Cre* mice to investigate the lineage commitment of mesenchymal stem cells. *Chfb $\beta$ <sup>ff</sup>/Osx-Cre* mice showed serious osteoporosis with a significant increase in adiposity [39]. Mice with an osteoprogenitor-specific *Dkk1* (encoding Dickkopf WNT signaling pathway inhibitor 1)



deletion presented an accumulation of bone marrow fat and a protected against cortical bone loss induced by a high-fat diet [40]. Using *Osx-Cre<sup>ERT2</sup>* mice, TSC complex subunit 2 (TSC2) haploinsufficiency in osteoprogenitors attenuated the increase in bone marrow fat [41].

However, there are several limitations of our study. The underlying mechanisms of how *CDC20* regulates adipogenic differentiation and the balance of bone-fat turnover were not fully determined. Additionally, whether *CDC20*

influences whole body fat accumulation requires examination in following studies, which would be significant in clinical applications.

### Conclusion

Overall, our study showed that *CDC20* knockdown increased adipogenic differentiation of BMSCs by decreasing  $\beta$ -catenin levels and induced adiposity accumulation in bone marrow. Furthermore, *CDC20* might be involved in

balancing adipogenesis and osteogenesis in stem cells in tissue engineering and as a therapeutic target in the treatment of osteoporosis.

#### Abbreviations

AM: Adipogenic medium;  $\alpha$ -MEM:  $\alpha$ -Minimum essential medium; APC/C: Anaphase-promoting complex/cyclosome; BMSCs: Bone marrow-derived mesenchymal stromal/stem cells; CDC20: Cell division cycle 20; DMEM: Dulbecco's modified eagle's medium; FBS: Fetal bovine serum; hASCs: Human adipose-derived stem cells; H&E: Hematoxylin and eosin; LiCl: Lithium chloride; NC: Negative control; Osx: Osterix; PM: Proliferation medium.

#### Supplementary Information

The online version contains supplementary material available at <https://doi.org/10.1186/s13287-022-03062-0>.

**Additional file 1: Fig. S1.** Knockdown of CDC20 enhances adipogenic differentiation of hASCs. **(A)** Fluorescence micrographs showing the lentivirus transduction efficiency. Scale bar, 500  $\mu$ m. **(B)** Relative mRNA expression of CDC20 in control shRNA (NC) and CDC20 knockdown (shCDC20-1, shCDC20-2) hASCs examined by qRT-PCR. **(C, D)** Oil red O staining **(C)** and quantification **(D)** of hASCs after adipogenic induction for 21 days. Scale bar, 100  $\mu$ m. All data are presented as the mean  $\pm$  SD ( $n=3$ , \*\*\*\* $p < 0.001$ ).

#### Acknowledgements

The authors are grateful to Dr. Yuan Zhu and Dr. Xuenan Liu for the help in animal experiments.

#### Author contributions

YD conducted the experiments, gathered and analyzed the data, and wrote the main manuscript text. YL, YZ, and PZ conceived the experiments, supervised the study, and edited the manuscript. All authors approved the final version of the manuscript.

#### Funding

The project was supported by the National Natural Science Foundation of China (81930026 to YZ and 81970911 to PZ), and the Beijing Municipal Science and Technology Commission (7182183 to YZ and 7202233 to PZ). The funding body had no role in the design of the study, in the collection, analysis, and interpretation of the data, and in writing the manuscript.

#### Availability of data and materials

All data generated or analyzed during this study are included in this published article.

#### Declarations

##### Ethics approval and consent to participate

Animals were supplied by the Biocytogen Co., Ltd. (Beijing, China) and Vital River Corporation (Beijing, China). All animal studies were approved by the Institutional Animal Care and Use Committee of the Peking University Health Science Center (LA2014233), and all experiments were carried out according to Institutional Animal Guidelines.

##### Consent for publication

Not applicable.

##### Competing interests

The authors declare no competing interests.

Received: 20 December 2021 Accepted: 4 June 2022

Published online: 02 September 2022

#### References

- Teitelbaum SL. Bone resorption by osteoclasts. *Science*. 2000;289(5484):1504–8.
- Chan GK, Duque G. Age-related bone loss: old bone, new facts. *Gerontology*. 2002;48(2):62–71.
- Tchkonina T, Giorgadze N, Pirtskhalava T, Tchoukalova Y, Karagiannides I, Forse RA, et al. Fat depot origin affects adipogenesis in primary cultured and cloned human preadipocytes. *Am J Physiol Regul Integr Comp Physiol*. 2002;282(5):R1286–96.
- Christodoulides C, Lagathu C, Sethi JK, Vidal-Puig A. Adipogenesis and WNT signalling. *Trends Endocrinol Metab*. 2009;20(1):16–24.
- Rosen ED, MacDougald OA. Adipocyte differentiation from the inside out. *Nat Rev Mol Cell Biol*. 2006;7(12):885–96.
- Muruganandan S, Roman AA, Sinal CJ. Adipocyte differentiation of bone marrow-derived mesenchymal stem cells: cross talk with the osteoblastogenic program. *Cell Mol Life Sci*. 2009;66(2):236–53.
- JafariNasabian P, Inglis JE, Reilly W, Kelly OJ, Ilich JZ. Aging human body: changes in bone, muscle and body fat with consequent changes in nutrient intake. *J Endocrinol*. 2017;234(1):R37–r51.
- Tontonoz P, Hu E, Spiegelman BM. Stimulation of adipogenesis in fibroblasts by PPAR $\gamma$ , a lipid-activated transcription factor. *Cell*. 1994;79(7):1147–56.
- Lin FT, Lane MD. CCAAT/enhancer binding protein  $\alpha$  is sufficient to initiate the 3T3-L1 adipocyte differentiation program. *Proc Natl Acad Sci U S A*. 1994;91(19):8757–61.
- Rosen ED, Spiegelman BM. Molecular regulation of adipogenesis. *Annual Rev Cell Dev Biol*. 2000;16:145–71.
- Mota de Sá P, Richard AJ, Hang H, Stephens JM. Transcriptional regulation of adipogenesis. *Compr Physiol*. 2017;7(2):635–74.
- Darlington GJ, Ross SE, MacDougald OA. The role of C/EBP genes in adipocyte differentiation. *J Biol Chem*. 1998;273(46):30057–60.
- Moseti D, Regassa A, Kim W-K. Molecular regulation of adipogenesis and potential anti-adipogenic bioactive molecules. *Int J Mol Sci*. 2016;17(1):124.
- Hartwell LH, Culotti J, Pringle JR, Reid BJ. Genetic control of the cell division cycle in yeast. *Science*. 1974;183(4120):46–51.
- Primorac I, Musacchio A. Panta rhei: the APC/C at steady state. *J Cell Biol*. 2013;201(2):177–89.
- Gayyed MF, El-Maqsoud NM, Tawfik ER, El Gelany SA, Rahman MF. A comprehensive analysis of CDC20 overexpression in common malignant tumors from multiple organs: its correlation with tumor grade and stage. *Tumour Biol*. 2016;37(1):749–62.
- Yang Y, Kim AH, Yamada T, Wu B, Bilimoria PM, Ikeuchi Y, et al. A Cdc20-APC ubiquitin signaling pathway regulates presynaptic differentiation. *Science*. 2009;326(5952):575–8.
- Wan L, Tan M, Yang J, Inuzuka H, Dai X, Wu T, et al. APC(Cdc20) suppresses apoptosis through targeting Bim for ubiquitination and destruction. *Dev Cell*. 2014;29(4):377–91.
- Kim EJ, Oh HY, Heo HS, Hong JE, Jung SJ, Lee KW, et al. Biological features of core networks that result from a high-fat diet in hepatic and pulmonary tissues in mammary tumour-bearing, obesity-resistant mice. *Br J Nutr*. 2013;110(2):241–55.
- Merhi Z, Polotsky AJ, Bradford AP, Buyuk E, Chosich J, Phang T, et al. Adiposity alters genes important in inflammation and cell cycle division in human cumulus granulosa cell. *Reprod Sci*. 2015;22(10):1220–8.
- Du Y, Zhang M, Liu X, Li Z, Hu M, Tian Y, et al. CDC20 promotes bone formation via APC/C dependent ubiquitination and degradation of p65. *EMBO Rep*. 2021;22(9): e52576.
- Maridas DE, Rendina-Ruedy E, Le PT, Rosen CJ. Isolation, culture, and differentiation of bone marrow stromal cells and osteoclast progenitors from mice. *J Vis Exp*. 2018. <https://doi.org/10.3791/56750>.
- Gimble JM, Zvonic S, Floyd ZE, Kassem M, Nuttall ME. Playing with bone and fat. *J Cell Biochem*. 2006;98(2):251–66.
- Takeda S, Eleftheriou F, Karsenty G. Common endocrine control of body weight, reproduction, and bone mass. *Annu Rev Nutr*. 2003;23:403–11.

25. Billon N, Dani C. Developmental origins of the adipocyte lineage: new insights from genetics and genomics studies. *Stem Cell Rev Rep*. 2012;8(1):55–66.
26. Qiu W, Andersen TE, Bollerslev J, Mandrup S, Abdallah BM, Kassem M. Patients with high bone mass phenotype exhibit enhanced osteoblast differentiation and inhibition of adipogenesis of human mesenchymal stem cells. *J Bone Miner Res*. 2007;22(11):1720–31.
27. Yu H. Cdc20: a WD40 activator for a cell cycle degradation machine. *Mol Cell*. 2007;27(1):3–16.
28. Liu X, Zhang F, Zhang Y, Li X, Chen C, Zhou M, et al. PPM1K regulates hematopoiesis and leukemogenesis through CDC20-mediated ubiquitination of MEIS1 and p21. *Cell Rep*. 2018;23(5):1461–75.
29. Quek LS, Grasset N, Jasmen JB, Robinson KS, Bellanger S. Dual role of the anaphase promoting complex/cyclosome in regulating stemness and differentiation in human primary keratinocytes. *J Invest Dermatol*. 2018;138(8):1851–61.
30. Abdallah BM, Kassem M. New factors controlling the balance between osteoblastogenesis and adipogenesis. *Bone*. 2012;50(2):540–5.
31. Peng XD, Xie H, Zhao Q, Wu XP, Sun ZQ, Liao EY. Relationships between serum adiponectin, leptin, resistin, visfatin levels and bone mineral density, and bone biochemical markers in Chinese men. *Clin Chim Acta*. 2008;387(1–2):31–5.
32. Gómez-Ambrosi J, Rodríguez A, Catalán V, Frühbeck G. The bone-adipose axis in obesity and weight loss. *Obes Surg*. 2008;18(9):1134–43.
33. Clevers H. Wnt/beta-catenin signaling in development and disease. *Cell*. 2006;127(3):469–80.
34. Li K, Mao Y, Lu L, Hu C, Wang D, Si-Tu J, et al. Silencing of CDC20 suppresses metastatic castration-resistant prostate cancer growth and enhances chemosensitivity to docetaxel. *Int J Oncol*. 2016;49(4):1679–85.
35. Zhang Q, Huang H, Liu A, Li J, Liu C, Sun B, et al. Cell division cycle 20 (CDC20) drives prostate cancer progression via stabilization of  $\beta$ -catenin in cancer stem-like cells. *EBioMedicine*. 2019;42:397–407.
36. Hadjihannas MV, Bernkopf DB, Brückner M, Behrens J. Cell cycle control of Wnt/ $\beta$ -catenin signalling by conductin/axin2 through CDC20. *EMBO Rep*. 2012;13(4):347–54.
37. Chu Z, Zhang X, Li Q, Hu G, Lian CG, Geng S. CDC20 contributes to the development of human cutaneous squamous cell carcinoma through the Wnt/ $\beta$ -catenin signaling pathway. *Int J Oncol*. 2019;54(5):1534–44.
38. Quach JM, Walker EC, Allan E, Solano M, Yokoyama A, Kato S, et al. Zinc finger protein 467 is a novel regulator of osteoblast and adipocyte commitment. *J Biol Chem*. 2011;286(6):4186–98.
39. Wu M, Wang Y, Shao JZ, Wang J, Chen W, Li YP. Cbf $\beta$  governs osteoblast-adipocyte lineage commitment through enhancing  $\beta$ -catenin signaling and suppressing adipogenesis gene expression. *Proc Natl Acad Sci U S A*. 2017;114(38):10119–24.
40. Colditz J, Picke AK, Hofbauer LC, Rauner M. Contributions of dickkopf-1 to obesity-induced bone loss and marrow adiposity. *JBM Plus*. 2020;4(6):e10364.
41. Ko FC, Kobelski MM, Zhang W, Grenga GM, Martins JS, Demay MB. Phosphate restriction impairs mTORC1 signaling leading to increased bone marrow adipose tissue and decreased bone in growing mice. *J Bone Miner Res*. 2021;36(8):1510–20.

## Publisher's Note

Springer Nature remains neutral with regard to jurisdictional claims in published maps and institutional affiliations.

Ready to submit your research? Choose BMC and benefit from:

- fast, convenient online submission
- thorough peer review by experienced researchers in your field
- rapid publication on acceptance
- support for research data, including large and complex data types
- gold Open Access which fosters wider collaboration and increased citations
- maximum visibility for your research: over 100M website views per year

At BMC, research is always in progress.

Learn more [biomedcentral.com/submissions](https://biomedcentral.com/submissions)

